

HIGH RESOLUTION AURORAL ABSORPTION MEASUREMENT WITH SCANNING-BEAM RIOMETER AT $L=6.1$

Hisao YAMAGISHI¹, Takashi KIKUCHI², Syuichi IKEDA³
and Takeo YOSHINO³

¹National Institute of Polar Research, 9-10, Kaga 1-chome, Itabashi-ku, Tokyo 173

²Hiraiso Solar-Terrestrial Research Center, Communications Research Laboratory,
3601, Isozaki, Nakaminato 311-12

³University of Electro-Communications, 5-1, Chofugaoka 1-chome, Chofu 182

Abstract: A multi-narrow-beam riometer system is in operation at Syowa Station, Antarctica since February 1985, to observe the cosmic radio noise absorption (CNA) with a spatial resolution of 10 km at 90 km altitude. This system, together with optical auroral observation at Syowa Station, enabled us to study the spatial relationship between visible aurora and auroral radio wave absorption with much better temporal and spatial resolution than previous studies.

The relationship was studied for different types of auroras, *i.e.*, (1) Poleward expanding arc in the evening hours, (2) Equatorward drifting arc embedded in homogeneous background aurora at midnight hours, and (3) Pulsating aurora in the post break-up phase. For case (1), a region of strong absorption was found to propagate poleward with a poleward expanding arc. However, the absorption area extended to the lower latitude side of a poleward-moving arc due to a longer remaining of the absorption even after the disappearance of visible aurora. For case (2), little absorption accompanied with discrete auroras. However, a better coincidence was found between absorption and homogeneous background aurora. For case (3), temporal variation of the both phenomena showed one-to-one correspondence, although the luminosity of auroras was much weaker than in the other cases.

1. Introduction

The relationship between visible aurora and auroral radio wave absorption has been studied since the beginning of 1960's with riometers and all-sky camera networks (BASLER, 1963; HOOK, 1968; BERKEY *et al.*, 1980) and multi-narrow-beam riometers along with photometers and all-sky cameras (KAVADAS, 1961; ANSARI, 1964; BERKEY, 1968; NIELSEN, 1980). The network observation dealt with large-scale auroral display, while multi-narrow-beam riometers detected small auroral structure within several tens of kilometers.

There are a variety of auroral display in different local times, and the features of associated absorption depend on the local time. BERKEY *et al.* (1980) used Alaskan riometer and all-sky camera chain data and found that, in the evening hours, diffuse aurora appeared with a weak absorption preceding a substorm onset. In the pre-midnight hours, a very intense absorption, lasting for a short time, accompanied westward traveling surges. Around midnight, an intense absorption was coincident with a poleward expanding bulge observed after a substorm onset. In the morning

hours, strong absorption events took place near the equatorward edge of the auroral oval associated with torchlike structure or patches in a diffuse aurora.

Based on a simultaneous observation with multi-narrow-beam riometers and photometers, directing 6° north and 6° south in zenith angle with field-of-view of 7° , BERKEY (1968) classified the observed absorption events into three categories defined as follows:

Category A: Intense 557.7 nm emission accompanying strong absorption

Category B: Intense emission accompanying very weak absorption

Category C: Weak emission accompanying strong absorption

Category A events often appear near the midnight, but can occur also in early evening hours during strong geomagnetic disturbances. Category B events occur mainly in the evening, while Category C events in the morning hours with eastward drifting patches of diffused aurora, or pulsating auroras.

A new riometer of high spatial resolution, *i.e.*, a scanning-beam riometer, was installed at Syowa Station (69.0°S , 39.6°E geographic; 66.1°S , 70.7°E geomagnetic; $L=6.1$), Antarctica (YAMAGISHI *et al.*, 1987; KIKUCHI *et al.*, 1988; YAMAGISHI and KIKUCHI, 1989). The ionospheric absorption within 60 km over Syowa Station in geomagnetic north-south and east-west directions can be measured with a spatial resolution of 10 km and temporal resolution of 10 s. In this report, some typical auroral absorption events observed by this new instrument are studied with better spatial and temporal resolution in comparison with previous studies.

2. Instrumentation

The riometer antenna system consists of phased array of coaxial colinear antennas similar to NIELSEN's system (1980). The antenna has two subarrays aligning along the geomagnetic north-south and east-west directions. Each array consists of 8 rows of 14 half-wave dipoles, which occupies the ground area of 50 m by 50 m for the receiving frequency of 30 MHz. The antenna has two scanning beams pointing to between $\pm 30^\circ$ in zenith angle in the north-south and east-west directions, along with four fixed beams pointing to the zenith and to the north, south and west with a zenith angle of 30° . These antenna beams have a width of 13° between half-power points, which cover an ionospheric region with a diameter of 20 km above the antenna and 27 km at a zenith angle of 30° . Figure 1 shows the cross sections of antenna beams at the absorption layer of 90 km altitude for two scanning beams (small open circles), four fixed-direction beams (hatched circles), and a broad beam of a conventional riometer (large circle).

The antenna beam scans the sky stepwise with an electrical switching of phase shifters in geomagnetic north-south and east-west directions at a speed of $6^\circ/\text{s}$, or 10 s/scan. Thus, the scanning beam illuminates an ionospheric area of 120 km in diameter with a spatial resolution of 10 km and a temporal resolution of 10 s. Four fixed-direction beams are connected to separate riometers (fixed-direction riometers) and used for higher time resolution (0.25 s) observation.

As to optical aurora observation, following instruments were available for this study at Syowa Station:

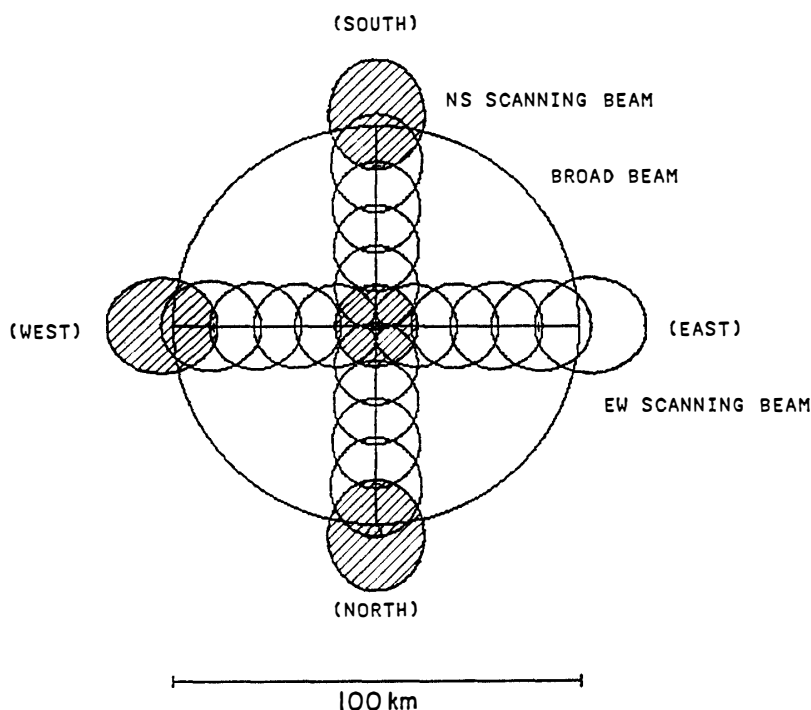


Fig. 1. Cross sections of the riometer antenna beams at the absorption layer at 90 km altitude, for two scanning beams (small open circles), four fixed-direction beams (hatched circles), and a broad beam of a conventional riometer (large circle).

Scanning photometer: 557.7 nm, field-of-view of 6° , scan speed 30 s in one way

Three-direction photometer: 427.8 nm, field-of-view of 7° , directing zenith, geomagnetically 30° north and 30° south

All-sky TV camera: Panchromatic

3. Observation

3.1 Absorption associated with poleward expanding arc

Figure 2 shows the records of a fluxgate magnetometer and broad-beam (beam-width 60°) riometer obtain at Syowa Station on March 25, 1986, when a local auroral break-up occurred at 1947 UT. The aurora observed by the all-sky TV camera showed a poleward shifting with a speed of 5.5 km/s, and the broad-beam riometer showed an abrupt increase of absorption amounting to 4.4 dB. The phenomenon during the time interval marked by vertical broken lines, was analyzed in detail with the scanning-beam riometer and optical observation instruments. A scanning photometer was in operation during this period, but the scanning speed of 30 s was insufficient for tracing a rapid auroral motion in this event. Therefore we utilized TV camera images to determine the auroral arc position.

Figure 3 shows a meridian-time display of the auroral arc sketched from the TV camera images (hatched areas) and the contour of associated auroral absorption observed by the scanning-beam riometer. The absorption intensity has not yet been finally calibrated, but the numerals on the contour roughly represent absorption

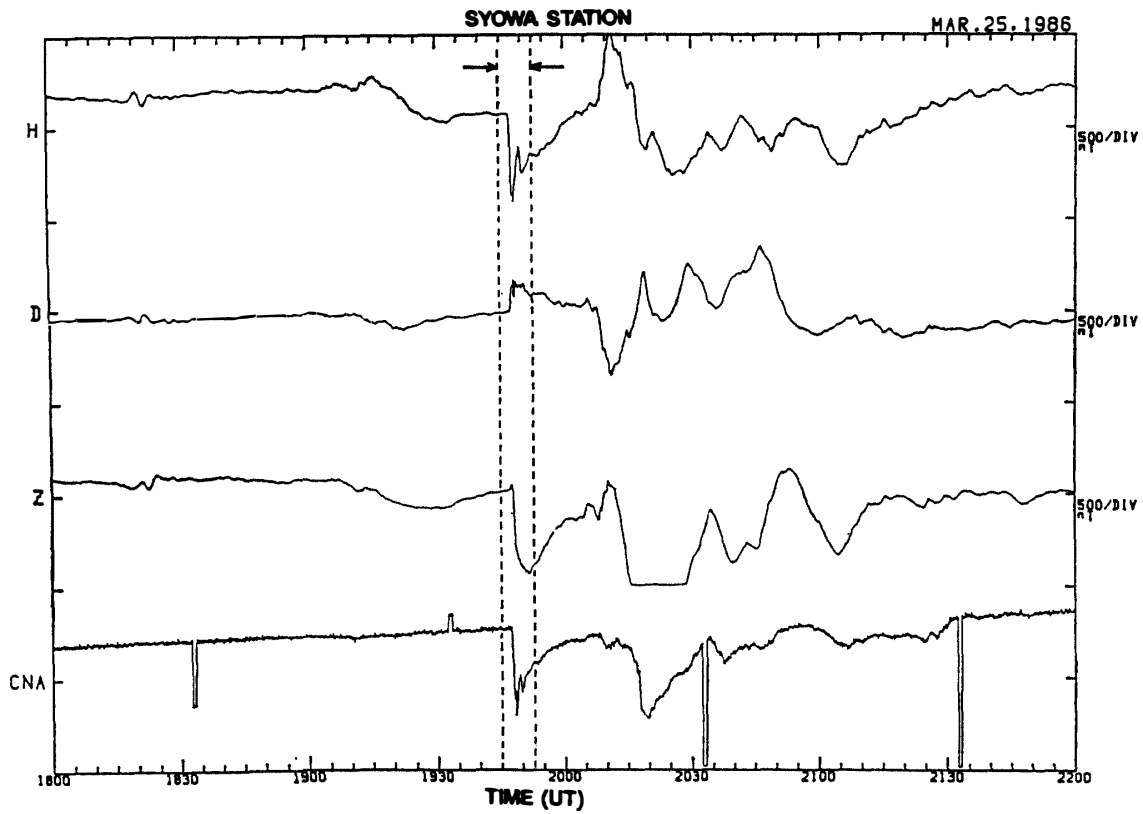


Fig. 2. Records of the three-component fluxgate magnetometer and broad-beam riometer at Syowa Station obtained in the evening of March 25, 1986. An extensive analysis was carried out for the time interval marked by vertical broken lines, when a local auroral break-up occurred, as shown in an extended time scale in Figs. 3 and 4.

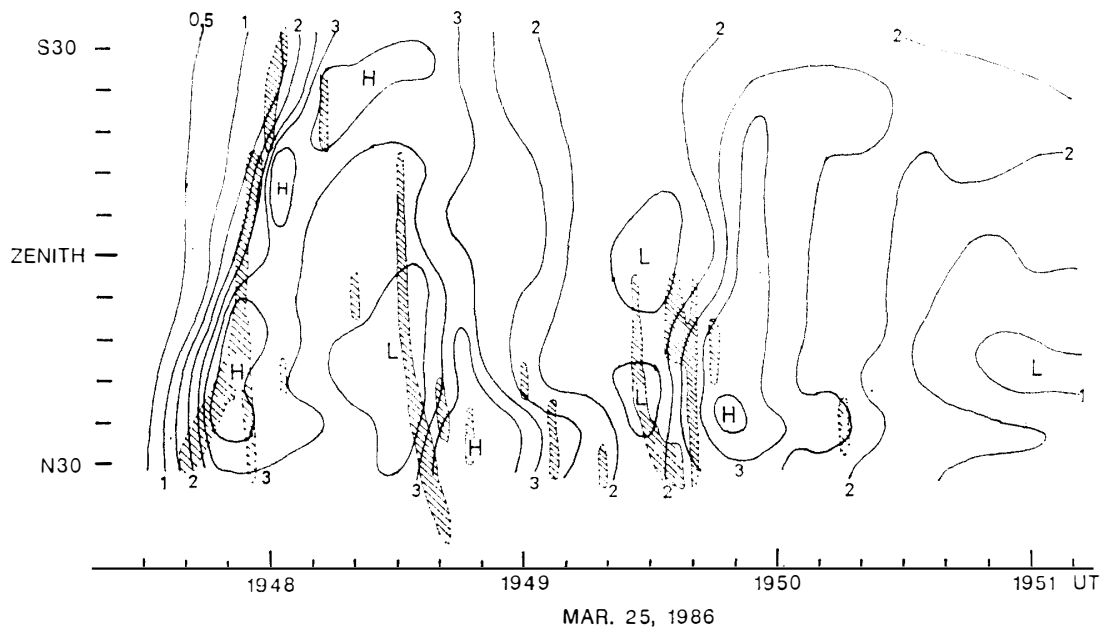


Fig. 3. A meridian-time display of the auroral arc sketched from all-sky auroral TV camera images (hatched area) and the contour of the associated auroral absorption observed by the scanning-beam riometer. The numerals on the contour roughly represent absorption in decibel.

in decibel. An intense auroral arc moved poleward at around 1948 UT, then returned equatorward at 1948:30. The auroral arc faded at around 1949 UT, and appeared again at 1949:30 in the northern sky. A region of strong auroral absorption showed similar displacement with auroral arcs. However, the area of the absorption region seems wider than the visual auroral arc, and the peak absorption was delayed by ~ 10 s after the appearance of the arc.

Because of a fixed beam-scan time of 10 s, the absorption contour may include a timing error of ± 10 s. In order to confirm whether the above-mentioned delay is an actual one, the temporal variations of auroral luminosity at 427.8 nm in three directions (30° south, zenith, and 30° north) are compared with the absorption for the same directions with a three-direction photometer and fixed-direction riometers. The results are shown in Fig. 4. In the figure, absorption increases are taken upward for an easy comparison with optical emission fluctuations. Vertical marks in the figure denote the same instants. The onset time of the absorption and the optical emission is almost the same, and the absorption peaks and the emission peaks

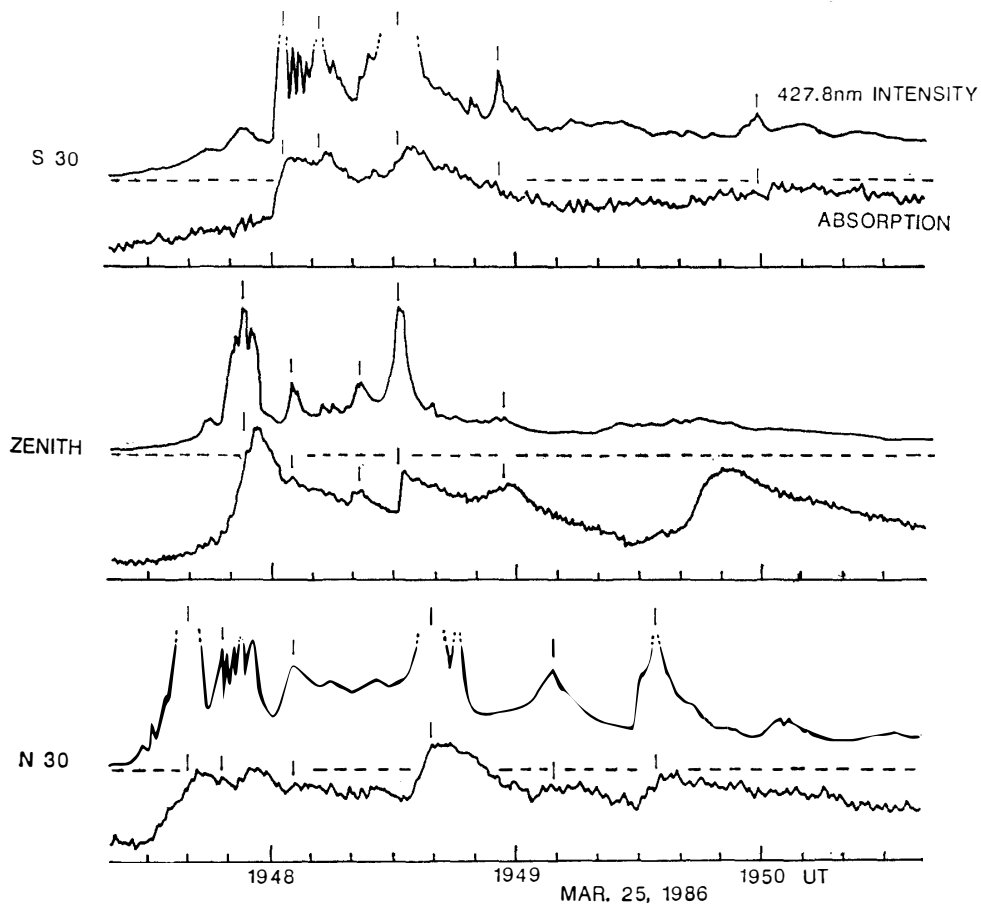


Fig. 4. Comparison of the time variation in 427.8 nm auroral intensity observed by the three-direction photometer (upper curves) and the absorption observed by the fixed-beam riometers (lower curves). The view directions of the both instruments were 30° south in zenith angle (top panel), zenith (middle panel) and 30° north (bottom panel). Vertical marks indicate the same time. The absorption is taken upward in the diagram.

occur almost simultaneously. However, the absorption always lasts much longer (10–20 s) than that of the visual emission. This causes an extension of the absorption area in the wake of moving auroral arcs. This is one reason why the absorption region is wider than the visual arc width, and the occurrence of the absorption seems to delay after the appearance of aurora in Fig. 3. A possible cause for a longer duration of the absorption will be discussed in section 4.

3.2 Absorption event at midnight

Absorption intensity with respect to aurora can change rapidly in both space and time even during an absorption event. An example is shown here. Figure 5 demonstrates the records of fluxgate magnetometer and broad-beam riometer obtained on May 2–3, 1986; a strong absorption amounting even to 6.6 dB occurred at 2305 UT. The scanning-beam riometer data were analyzed for the time interval marked by broken lines, which includes this specific event. Auroral image from all-sky TV camera in this period showed that an equatorward drifting arc was embedded in homogeneous background for the time interval of 2306–2315 UT. Auroral activity calmed down during 2315–2320 UT, then pulsative aurora appeared for the period of 2320–2340 UT.

In order to obtain the temporal and spatial relationship between visible aurora and riometer absorption, a meridian-time contour is displayed for the time interval

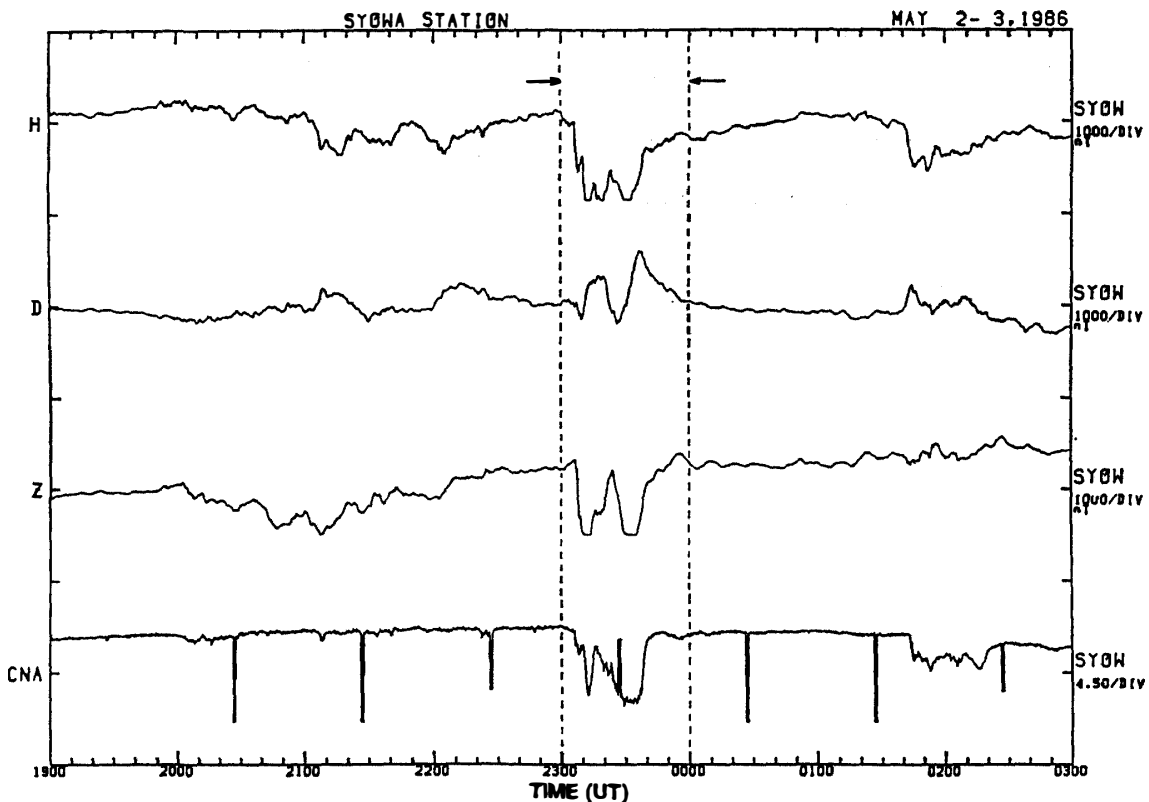


Fig. 5. Records of the fluxgate magnetometer and the broad-beam riometer at Syowa Station at geomagnetically disturbed period during the night of May 2–3, 1986. Time period marked by vertical broken lines is the interval for analysis in Figs. 6–9.

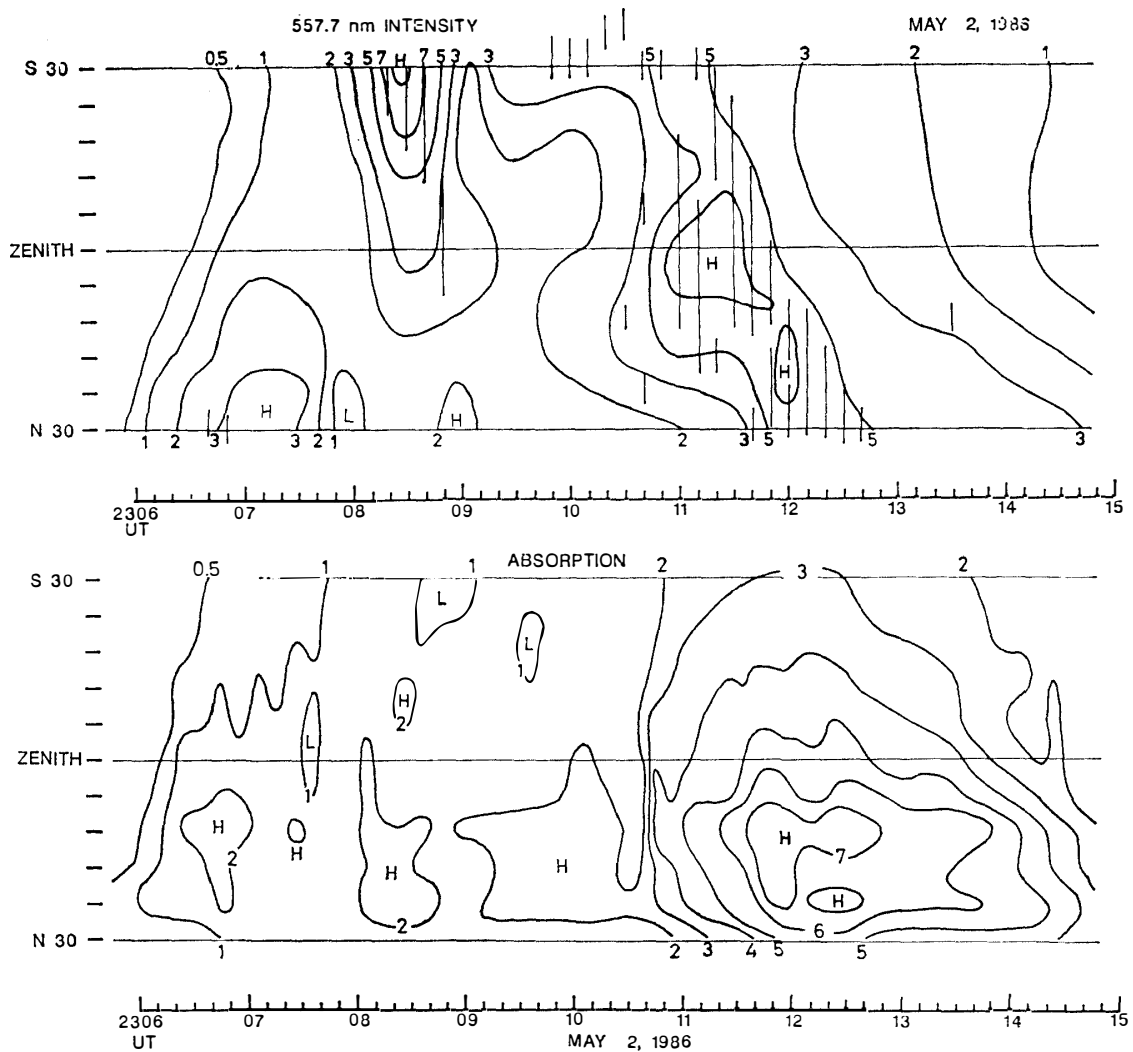


Fig. 6. A meridian-time contour displays of 557.7 nm auroral intensity obtained from the scanning photometer (upper panel) and the auroral absorption obtained from the scanning-beam riometer (lower panel). Vertical lines in the upper panel indicate the location of discrete auroras obtained from the all-sky auroral TV camera images.

of 2306–2315 UT as shown in Fig. 6. Presented in the upper panel is the contour of 557.7 nm intensity, where the vertical lines indicate the locations of discrete auroras and the numerals on the contour roughly represent the intensity in kR. The lower panel shows the absorption with the contour in decibel. The general trend of the both phenomena shows good similarity. However, little correspondence is found between discrete aurora and absorption, especially at the time interval of 2308–2309 UT. This will suggest that precipitating electrons causing discrete aurora seem to contribute little to absorption. This seems to come from the fact that the discrete aurora is caused principally by mono-energetic electrons of several keV energy (LUI *et al.*, 1977), while the auroral absorption is mainly caused by electrons of much higher energy, say several tens of keV (PENMAN *et al.*, 1979).

The absorption seemed to have a better correspondence with homogeneous

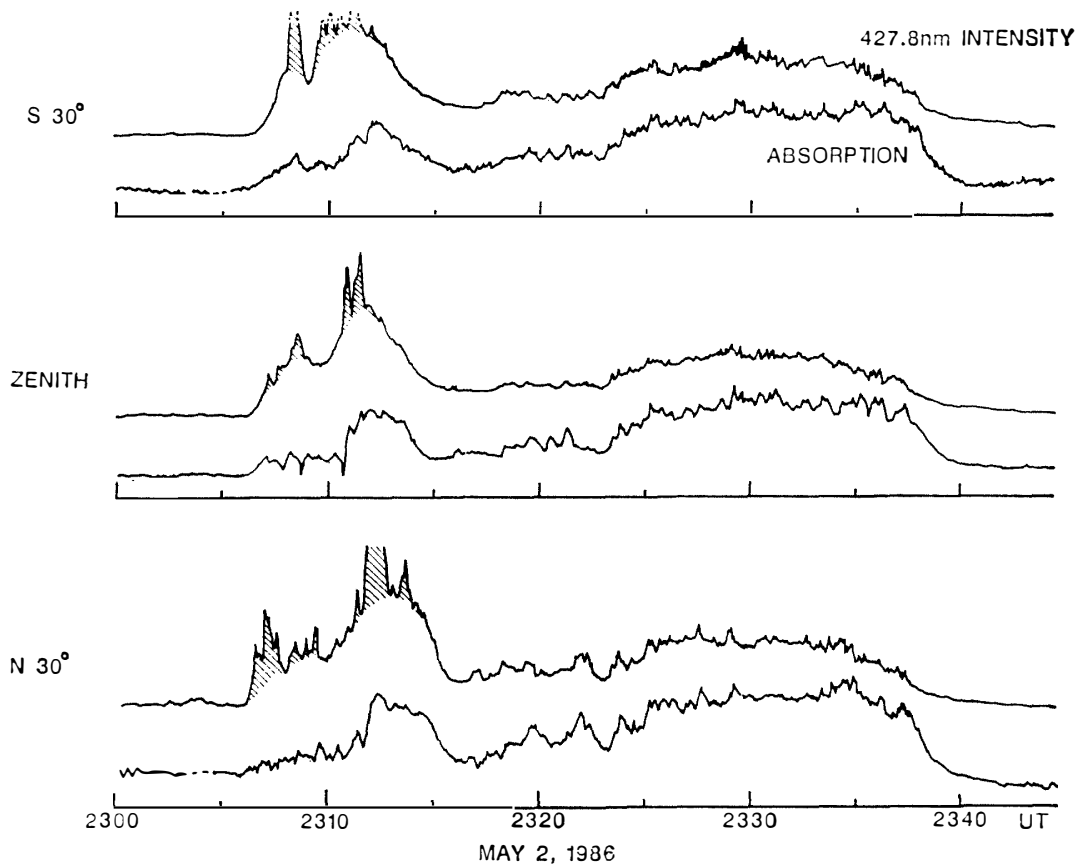


Fig. 7. Comparison between auroral intensity at 427.8 nm and absorption observed in the directions of 30° south, 0° and 30° north in zenith angle by the three-direction photometer and the fixed-beam riometers for the period of 2300–2345 UT on May 2, 1986. Hatched areas on the curves of auroral intensity indicate the contributions from discrete auroras in all-sky TV camera images.

aurora in the background. Figure 7 compares the auroral intensity at 427.8 nm and the absorption observed in the directions of 30° south, zenith and 30° north in zenith angle by the three-direction photometer and fixed-direction riometers. The shaded parts of auroral intensity curves are contributed from discrete auroras recognized in all-sky TV camera images and the rest of the auroral intensity comes from homogeneous aurora in the background. Except for these shaded parts, the temporal variations of the auroral intensity and the absorption are in good agreement with each other for the time interval of 2306–2315 UT. This fact suggests that the homogeneous aurora in the background and the auroral absorption originated from the same high energy electrons accelerated in the plasmasheet at the substorm time (McILWAIN, 1975).

Temporal variation of auroral intensity and absorption showed a remarkable agreement for the time period of 2320–2340 UT when pulsating auroras appeared in the sky. The emission intensity, however, became much weaker and the absorption intensity greatly enhanced than the preceding period of 2306–2315 UT. This feature indicates that the energy spectrum of precipitating electrons became harder after 2320 UT. Hence, it can be thought that the precipitation in this period was not

attributable to direct injection from the plasmashet, but caused by pitch angle scattering of trapped electrons drifting to the morning side.

4. Discussion

Intensity ratio between aurora and auroral absorption changes significantly for different type of aurora as demonstrated in Fig. 6. This is due to the fact that auroral optical emission is mainly caused by precipitating electrons of several keV, while the absorption is effectively caused by much higher energy electrons of several tens of keV (PENMAN *et al.*, 1979). Therefore, a change in the characteristic energy of precipitating electrons affects the intensity ratio between the two phenomena. JOHANSEN (1965) introduced a ratio between auroral absorption A (dB), and the square root of auroral intensity at 557.7 nm, $\sqrt{I(\text{kR})}$, as a measure of characteristic energy of precipitating electrons from the following reason. A is proportional to the ionospheric electron density N_e , and N_e is proportional to the square root of ionization rate q in equilibrium state. As q is proportional to I , the ratio A/\sqrt{I} is independent of electron flux intensity and depends only on the energy of the precipitating electrons in a manner that A/\sqrt{I} increases for harder energy spectrum. BAILEY (1968) calculated relationship between A/\sqrt{I} and e -folding energy E_0 of precipitating electron spectrum based on the observational data by EATHER and JACKA (1966).

Thus, it is possible to obtain a spatial change of the characteristic energy of auroral electrons by calculating A/\sqrt{I} values in each field-of-view direction of the scanning-beam riometer and the scanning photometer.

As an example, A/\sqrt{I} values are calculated for the absorption event described in 3.2, in which the characteristic energy is expected to change rapidly in time and space. Figure 8 shows time variations of auroral intensity at 557.7 nm (upper panel) observed in eleven directions at every 6° in zenith angle from 30° south to 30° north, and the absorption observed by the scanning-beam riometer (lower panel) in the same eleven directions. Presented in Fig. 9 are time variations of the calculated A/\sqrt{I} values for the same eleven directions as in Fig. 8. A thin horizontal line in each panel indicates the ratio of unity. The ratio A/\sqrt{I} shows a marked temporal variation from ~ 0.3 in the period of 2306–2311 UT when discrete aurora appeared in the southern sky, to ~ 1.0 at around 2313 UT when homogeneous aurora appeared, to more than 1.0 after 2325 UT when pulsating aurora appeared. A/\sqrt{I} values in the period of 2317–2320 UT is less reliable because both A and I values are small. Based on A/\sqrt{I} values, the absorptions in the above three time intervals are classified into Category B, A and C of Berkey's definition as shown in the top of the figure. According to the relationship between A/\sqrt{I} and E_0 calculated by BAILEY (1968), e -folding energy of precipitating electrons for the above three period is estimated to be ~ 5 keV, ~ 20 keV, and 20–40 keV, respectively.

It should be noted that A/\sqrt{I} shows a significant difference in the north-south direction. For example, A/\sqrt{I} is small in the southern directions during 2306–2311 UT, when a discrete aurora appeared in the southern sky, and A/\sqrt{I} becomes larger in the northern directions (low latitude side) during 2325–2339 UT, when pulsating

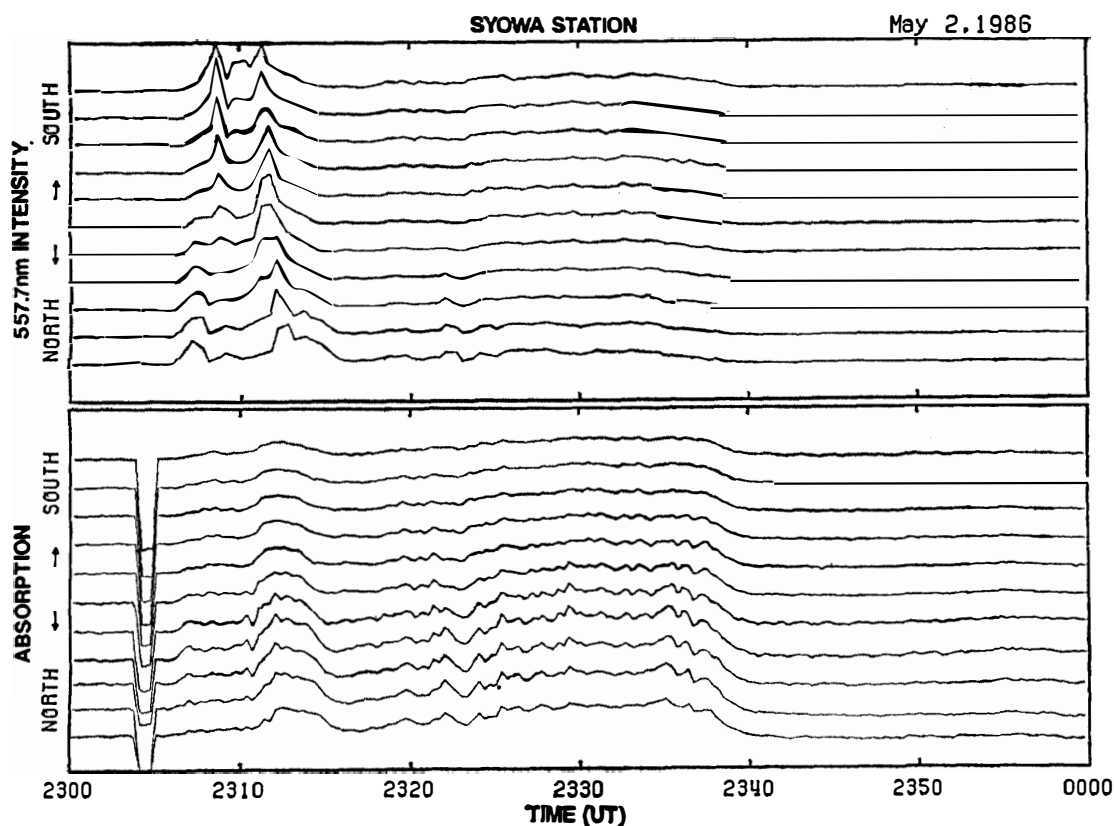


Fig. 8. Time variations of 557.7 nm auroral intensity observed by the scanning photometer (upper panel) and the auroral absorption observed by the scanning-beam riometer (lower panel). Eleven curves in each panel are obtained for different directions every 6° apart in zenith angle from 30° south to 30° north. The absorption increase is taken upward in the diagram.

aurora appeared. The observed spatial variation of A/\sqrt{I} values suggests that the characteristic energy of auroral electrons changes considerably within a narrow area of 120 km. These small scale changes of electron spectral features were averaged and overlooked in previous broad-beam riometer observations.

Absorption observed in the evening to midnight hours showed a temporal feature of abrupt increase and slow decrease as illustrated in Fig. 4. In the figure, the absorption lasted even after the disappearance of strong optical emission of discrete aurora. There are two possibilities to explain the above slow decreasing feature; the one is to explain it in terms of ionospheric time constant, and the other by temporal and spatial change of precipitating electron energy spectrum.

As the former explanation, the ionospheric time constant τ is given by $\tau \sim 1/2\alpha N_0$, where α denotes the effective recombination coefficient and N_0 the ionospheric electron density at an altitude of the absorption layer. As α and N_0 are functions of altitude (BAILEY, 1968), τ depends on altitude of the absorption layer in a manner that τ increases for higher absorption altitude. In previous works, τ was obtained from a calculation (REID and PHILLIPS, 1971) and observations (REID and PHILLIPS, 1971; ARNOLDY *et al.*, 1982) for pulsating auroras. They obtained a time constant

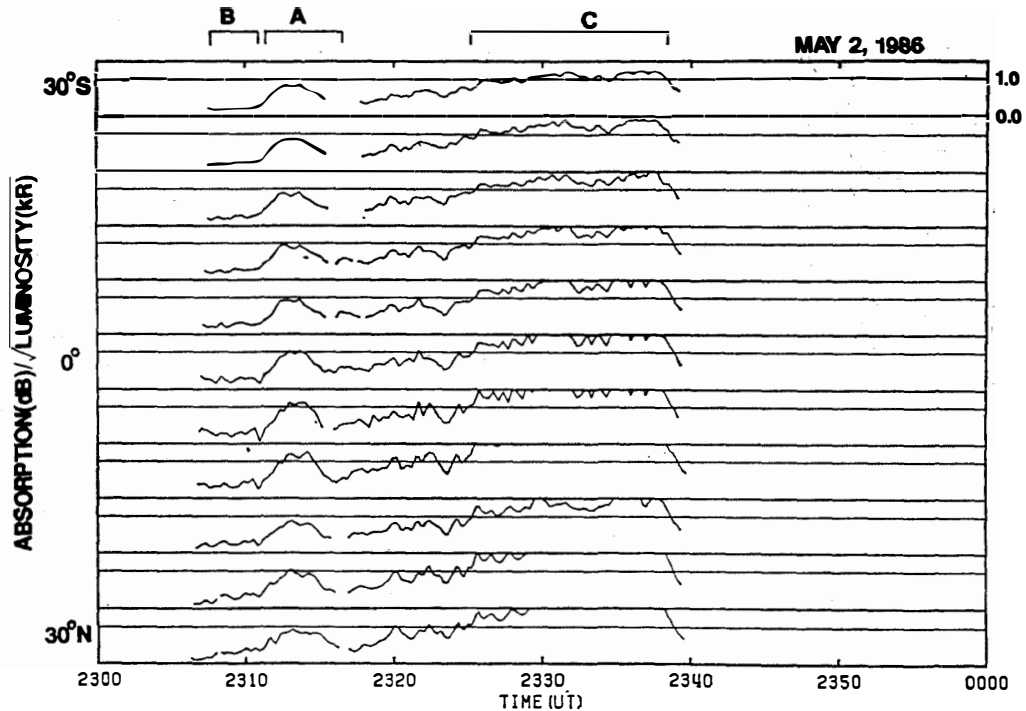


Fig. 9. Time variations of the ratio between absorption intensity in dB and square root of auroral luminosity in kR calculated for the absorption event shown in Fig. 8. Eleven curves in each panel are obtained for different directions every 6° apart in zenith angle from 30° south to 30° north. Absorption feature changes rapidly from Category A (of Berkeley's classification) at 2307–2311 UT to Category B at 2312–2316 UT, and to Category C at 2325–2339 UT.

of ~ 5 s. Our observational results, however, showed much longer decay time of 10–20 s. The above difference can be attributed to the fact that a characteristic energy of precipitating electrons is lower in break-up auroras than in pulsating auroras, and an altitude of the absorption layer is expected to be higher and the time constant longer in break-up auroras.

The latter explanation is also possible from the fact that the optical emission shown in Fig. 4 did not reach a base line level when a discrete aurora disappeared from the photometer field-of-view. This fact suggests that a sudden decrease of optical emission only means a decrease in low energy (several keV) part of auroral electrons, and higher energy (several tens of keV) electrons still precipitated after disappearance of the discrete aurora and caused weak optical emission and strong absorption. It is likely that the both processes mentioned above worked together to cause a slow decreasing of the break-up time absorption.

5. Summary

From the simultaneous observation of the optical aurora and auroral absorption by photometers, all-sky TV camera and the multi-narrow-beam riometer at Syowa Station, the relationship between the both phenomena was obtained with better spatial and temporal resolution than in previous studies. The following are our

observational results.

- (1) A region of strong auroral absorption was found to propagate poleward in association with poleward expanding arc in the premidnight. A longer remaining of the absorption after the disappearance of visible aurora caused an extension of the absorption area on the lower latitude side of a poleward-moving arc.
- (2) Around the midnight, a discrete aurora is associated with little absorption, while the background homogeneous aurora shows good spatial and temporal correlation with the absorption.
- (3) The temporal variations of pulsating aurora intensity and of riometer absorption showed one-to-one correspondence with each other, although the auroral luminosity was much weaker and the absorption intensity much stronger in comparison with those appeared before midnight.

It was found that the energy spectrum of precipitating electrons changes rapidly in time (in a few tens of minutes) and in space (several tens of kilometers), and this is the reason why better temporal and spatial resolution is required in the auroral absorption observation.

Acknowledgments

The authors wish to express their sincere appreciation to the wintering members of the 26th and 27th Japanese Antarctic Research Expedition for their efforts in the construction and operation of this riometer system at Syowa Station. We also express our heartfelt thanks to Professors T. HIRASAWA, M. EJIRI, H. FUKUNISHI and N. SATO for continuous encouragement for the present work.

References

- ANSARI, Z. A. (1964): The aurorally associated absorption of cosmic noise at College, Alaska. *J. Geophys. Res.*, **69**, 4493–4513.
- ARNOLDY, R. L., DRAGOON, K., CAHILL, L. J., Jr., MENDE, S. B. and ROSENBERG, T. J. (1982): Detailed correlations of magnetic field and riometer observations at $L=4.2$ with pulsating aurora. *J. Geophys. Res.*, **87**, 10449–10456.
- BAILEY, D. K. (1968): Some quantitative aspects of electron precipitation in and near the auroral zone. *Rev. Geophys.*, **6**, 289–346.
- BASLER, R. P. (1963): Radio wave absorption in the auroral ionosphere. *J. Geophys. Res.*, **68**, 4665–4681.
- BERKEY, F. T. (1968): Coordinated measurements of auroral absorption and luminosity using the narrow beam technique. *J. Geophys. Res.*, **73**, 319–337.
- BERKEY, F. T., ANGER, C. D., AKASOFU, S.-I. and RIEGER, E. P. (1980): The signature of large-scale auroral structure in radio wave absorption. *J. Geophys. Res.*, **85**, 593–606.
- EATHER, R. H. and JACKA, F. (1966): Auroral absorption of cosmic radio noise. *Aust. J. Phys.*, **19**, 215–239.
- HOOKE, J. L. (1968): Morphology of auroral zone radiowave absorption in the Alaska sector. *J. Atmos. Terr. Phys.*, **30**, 1341–1351.
- JOHANSEN, O. E. (1965): Variations in energy spectrum of auroral electrons detected by simultaneous observation with photometer and riometer. *Planet. Space Sci.*, **13**, 225–235.
- KAVADAS, A. (1961): Absorption measurements near the auroral zone. *J. Atmos. Terr. Phys.*, **23**, 170–176.

- KIKUCHI, T., YAMAGISHI, H. and SATO, N. (1988): Eastward propagation of Pc 4–5 range CNA pulsations in the morning sector observed with scanning narrow beam riometer at $L=6.1$. *Geophys. Res. Lett.*, **15**, 168–171.
- LUI, A. T. Y., VENKATESAN, D., ANGER, C. D., AKASOFU, S.-I., HEIKKILA, W. J., WINNINGHAM, J. D. and BURROWS, J. R. (1977): Simultaneous observations of particle precipitations and auroral emissions by the ISIS 2 satellite in the 19–24 MLT sector. *J. Geophys. Res.*, **82**, 2210–2226.
- McILWAIN, C. E. (1975): Auroral electron beams near the magnetic equator. *Physics of the Hot Plasma in the Magnetosphere*, ed. by B. HULTQVIST and L. STENFLO. New York, Plenum Press, 91–112.
- NIELSEN, E. (1980): Dynamics and spatial scale of auroral absorption spikes associated with the substorm expansion phase. *J. Geophys. Res.*, **85**, 2092–2098.
- PENMAN, J. M., HARGREAVES, J. K. and McILWAIN, C. E. (1979): The relation between 10 to 80 keV electron precipitation observed at geosynchronous orbit and auroral radio absorption observed with riometers. *Planet. Space Sci.*, **27**, 445–451.
- REID, J. S. and PHILLIPS, J. (1971): Time lags in the auroral zone ionosphere. *Planet. Space Sci.*, **19**, 959–969.
- YAMAGISHI, H., KIKUCHI, T., IKEDA, S. and SATO, N. (1987): Initial results of scanning-beam riometer observation at Syowa Station; Relationship between the size of absorption region and the intensity ELF/VLF emission on the ground. *Proceedings of Chapman Conference on Plasma Waves and Instabilities in Magnetosphere and Comets*, ed. by H. OYA and B.T. TSURUTANI. Sendai, Committee on Sendai Chapman Conference, 230–233.
- YAMAGISHI, H. and KIKUCHI, T. (1989): Souten-gata riomêta no kaihatsu (Development of scanning narrow beam riometer). *Nankyoku Shiryô (Antarct. Rec.)*, **33**, 17–32.

(Received November 2, 1988; Revised manuscript received February 25, 1989)